Available online at www.sciencedirect.com
SCIENCE DIRECT®
Bioorganic & Medicinal Chemistry 13 (2005) 5909–5914
Bioorganic & Medicinal Chemistry

Novel synthetic isoquinolino[5,4-*ab*]phenazines: Inhibition toward topoisomerase I, antitumor and DNA photo-cleaving activities

Peng Yang,[a] Qing Yang,[b] Xuhong Qian[a,c,*] and Jingnan Cui[a]

[a]*State Key Laboratory of Fine Chemicals, Dalian University of Technology, Dalian 116012, China*
[b]*Department of Bioscience and Biotechnology, Dalian University of Technology, Dalian 116012, China*
[c]*Shanghai Key Laboratory of Chemical Biology, East China University of Science and Technology, Shanghai 200237, China*

Received 15 June 2005; revised 10 July 2005; accepted 12 July 2005
Available online 22 August 2005

Abstract—The novel DNA interactive isoquinolino[5,4-*ab*]phenazine derivatives were designed and synthesized. Their inhibitory abilities toward topoisomerase I, antitumor activities and DNA photo-cleaving abilities were examined. The substituents at *peri* sites of two phenazine N atoms played very important roles for all these biological activities. At a concentration of 100 μM, all these phenazine derivatives (but **A2** and **A6**) exhibited an inhibitory activity toward topoisomerase I. **A6** had efficient antitumor activities against both human lung cancer cell (A549) and murine leukemia cell (P388). **A1**, **A5**, and **A6** exhibited antitumor activities selectively only against P388. **A2** was the most efficient DNA photocleaver, which had converted supercoiled DNA from form I to form II at <1 μM. Under anaerobic conditions, the electron transfer mechanism mainly contributed to DNA photo-induced cleavage, while under aerobic conditions, superoxide anion was also involved in this process.

1. Introduction

DNA intercalators have received much attention due to their therapeutic potential in anticancer treatment.[1] Some of these compounds, known as photonucleases, cleave DNA under light irradiation of a certain wavelength,[2] and also exhibit inhibitory activity against DNA regulatory enzymes, such as topoisomerase I.[3] Either DNA damage or topoisomerase inhibition is believed to disrupt DNA replication in vivo and thus, in turn, to show the cytotoxicity against tumor cells. Therefore, any development in the design of DNA intercalators with high topoisomerase inhibition, antitumor and DNA photo-cleaving activities is of the importance.

Various attempts have been made to modify the naphthalimide and phenazine units to promote their topoisomerase I inhibitory, antitumor and DNA photo-damaging abilities. Most of these works are focused on incorporating substituents or fusing five- or six-membered (phenyl or heterocyclic) rings to the naphthalene skeletons.[3] Brana's group made a lot of effort to improve naphthalimide derivatives' topoisomerase inhibitory and antitumor abilities.[4] Fernández et al.[5] reported a photosensitive DNA cleaver containing the phenazine bisintercalator. Gamage et al.[6] found that the heterocyclic phenazinecarboxamides could be used as topoisomerase-targeted anticancer agents. Studying the DNA-binding property of dipyrido [3,2-*a*: 2′,3′-*c*]phenazine (dppz) unit, Phillips et al.[7] found that intramolecular charge transfer accounted for unstructured luminescence. However, examples that took advantage of the structural characteristics of both naphthalimide and phenazine chromophores seldom appeared (see Figure 1).

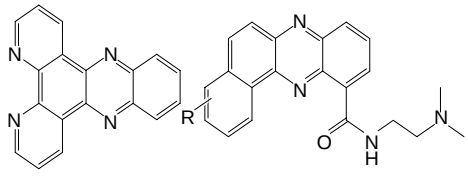

Figure 1. Structures of the reported phenazine derivatives.

Keywords: Phenazine naphthothiazole carboxamides; Photocleavage; Cytotoxicity.
* Corresponding author. Tel.: +86 411 83673466; fax: +86 411 83673488; e-mail addresses: xhqian@dlut.edu.cn; xhqian@ecust.edu.cn

0968-0896/$ - see front matter © 2005 Elsevier Ltd. All rights reserved.
doi:10.1016/j.bmc.2005.07.029

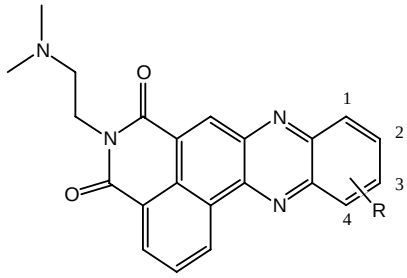

Figure 2. Structures of the novel isoquinolino[5,4-*ab*]phenazine.

In our continuous attempt[8] to develop compounds with high DNA-binding affinity and highly active antitumor activities, we designed and synthesized novel isoquinolino[4,5-*bc*]phenazine derivatives **A1**–**A6** (Fig. 2). In this study, naphthalimide active group remained in the structure and the quinoxaline unit was effectively fused with the electron-deficient naphthalimide.

These compounds were designed to include the obvious electron-deficient characteristics for the sake of strong electron-withdrawing effects of two carbonyl groups of naphthalimide. In addition, their asymmetrical electron-withdrawing effects exert different actions on the electrons of phenazine N heteroatoms. Hence, highly DNA intercalative abilities of these novel phenazine derivatives, their antitumor activities, and DNA photo-damaging properties were anticipated.

2. Results and discussion

2.1. Synthesis and spectra

The synthesis of compounds **A1**–**A6** is shown in Scheme 1. Take compound **A1** as an example: the starting material, 4-bromo-3-nitro-1, 8-naphthalic anhydride, reacted with aniline in DMF at room temperature for 5 h. And then, the ring closure reaction was carried out based on the reported procedure.[9] The obtained naphthalic anhydride was condensed with *N*,*N*-dimethylethylenediamine in ethanol for 2 h to give the designed compounds. After separation with careful column chromatography, each pure targeted product was obtained. All their structures were confirmed by ^{1}H NMR, HRMS, and IR.

Table 1. UV–vis and fluorescent data of **A1**–**A6**[a,b]

Compounds	UV λ_{max}, nm (lgε)	FL λ_{max}, nm (Φ)
A1	374(3.66)	430(0.00065)
A2	384(3.04)	454(0.00082)
A3	423(3.33)	483(0.02265)
A4	410(3.38)	467(0.00100)
A5	420(3.28)	480(0.00717)
A6	378(3.31)	455(0.00145)

[a] In absolute ethanol.
[b] With rhodamine B in ethanol as quantum yield standard (Φ = 0.97).

Table 1 shows the UV–vis and fluorescent data of **A1**–**A6**. It can be seen that the fluorescence quantum yields of these compounds were relatively low, which may have been caused by the rapid IST from a singlet to the triplet. The compound **A3**, due to the existence of a methoxyl group at the 1-site, had a relatively higher fluorescence quantum yield compared to other compounds.

The Scatchard-binding constant between the compound **A2**, used as an example, and calf thymus DNA was determined using the fluorescence technique method (Fig. 3).[10] Its Scatchard-binding constant was 3.63×10^5 M^{-1}, which indicated that **A2** could effectively intercalate into the calf thymus DNA.

2.2. Topoisomerase I inhibitory and antitumor activities

The inhibitory activities of these compounds toward topoisomerase I were evaluated by 2% agarose-gel

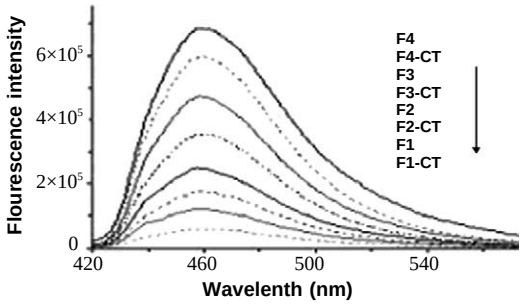

Figure 3. Fluorescent spectra before and after interaction of compound **A2** with calf thymus DNA. Curves F and F-CT correspond to compound **A2** before and after being mixed with DNA.

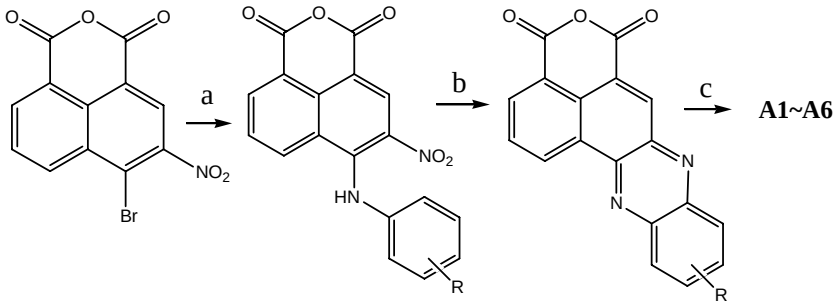

Scheme 1. Synthesis of **A1**–**A6**. Reagents and conditions: (a) aniline derivatives, DMF, room temperature, 5 h; (b) $NaBH_4$, NaOH, H_2O, reflux for 24 h; (c) *N*,*N*-dimethylethylenediamine, ethanol, reflux for 2 h.

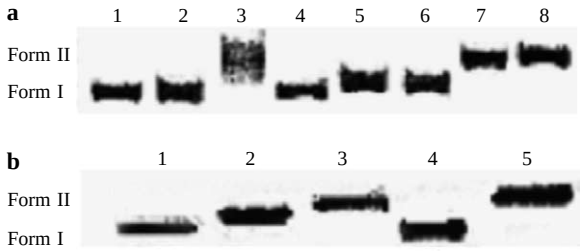

Figure 4. (a) Inhibition of the relaxation activity of topoisomerase I by **A1**–**A6** (100 μM). Supercoiled pBR322 DNA was relaxed by incubating with topoisomerase I. Lane 1, DNA alone; lanes 2–7, compounds **A1**, **A2**, **A3**, **A4**, **A5**, **A6** + DNA + Topo I, respectively; lane 8, DNA + Topo I; (b) inhibition of the relaxation activity of topoisomerase I by compound **A3**. Lane 1, DNA + Topo I + **A3** (50 μM); lane 2 DNA + Topo I + **A3** (20 μM); lane 3, DNA + Topo I + **A3** (10 μM); lane 4, DNA alone; lane 5, DNA + Topo I.

electrophoresis (Fig. 4). As shown in Figure 4a, **A1**–**A6** (100 μM) displayed a different inhibitory activity in the order: **A1** ≈ **A3** > **A4** ≈ **A5** > **A6** ≈ **A2**. **A2** was almost inactive, even at a concentration of 100 μM (Fig. 4a, lane 3). However, **A3** could inhibit topoisomerase I at the minimized concentration of 20 μM (Fig. 4b). Compared with **A2**, **A3** displayed a stronger inhibitory activity toward topoisomerase I. This result indicated that the oxygen atom at the 1-site might favor the binding between **A3** and its corresponding receptor. However, for 2-site-substituted compounds (**A4** and **A5**), there was no obvious difference between their weaker inhibitory activities. These results suggested that substituted sites affected greatly the inhibitory activity toward topoisomerase I.

The antitumor activities in vitro of all these isoquinolino[5,4-*ab*]phenazine derivatives were evaluated against cell lines of human lung cancer cell (A549) and murine leukemia cell (P388), respectively. The results are given in Table 2. The IC_{50} value represents the drug concentration (μM) required to inhibit the cell growth by 50%. **A6** showed the most efficient activities against P388 (IC_{50}, 0.33 μM) cell, while **A4** exhibited the highest activities against A549 (IC_{50}, 1.51 μM). For A549, the order of cytotoxicity exhibited by these compounds was: **A4** > **A6** > **A2** > **A1** > **A3** > **A5**, while the order of their cytotoxic potency against P388 was as follows: **A6** > **A1** > **A4** ≈ **A5** > **A3** > **A2**. The selectivity of the antitumor activities of **A1**, **A5**, and **A6** was also observed. **A1** was 11-fold more cytotoxic against P388 than against A549, **A5** was 12-fold, and **A6** was 5-fold, reflecting their different activities toward human or lung cell type.

Table 2. Cytotoxicities of **A1**–**A6**

Compounds	Cytotoxicity (IC_{50}, μM)	
	A549[a]	P388[b]
A1	5.16	0.46
A2	3.79	7.25
A3	7.03	2.54
A4	1.51	1.04
A5	12.0	1.02
A6	1.92	0.33

[a] Cytotoxicity (CTX) against human lung cancer cell (A549) was measured by sulforhodamine B dye-staining method.[11]

[b] CTX against murine leukemia cells (P388) was measured by microculture tetrazolium-formazan method.[12]

Based on these results, we did not find any obvious relationship between the cytotoxic potency of **A1**–**A6** and their topoisomerase I inhibitory activities. However, there was a trend that was worth noting here. The compound **A6** with a methyl group at the 4-site exhibited decent activity for both A549 and P388. Rewcastle[9] has once showed that introduction of a methyl group *peri* to the phenazine N atoms enhanced antitumor activity in their assay toward P388 leukemia and Lewis lung carcinoma cell lines. For phenazine N atoms in this study, there were two *peri* sites, 1-site (**A2** and **A3**) and 4-site (**A6**). Against the two tested cancer cells, **A6** exhibited a higher cytotoxicity than what **A2** and **A3** did, suggesting that these two *peri*-substituted compounds exhibited quite different effects on their antitumor activities.

2.3. DNA photo-damaging property

The photo-induced DNA cleaving activities of **A1**–**A6** were assayed using supercoiled pBR322 DNA. As shown in Figure 5a, **A1**–**A6** caused DNA cleavage under the irradiation of 365 nm-UV light, confirming that the UV light functioned as a trigger to initiate DNA strand scission. **A2** with a methyl group at the 1-site, a *peri* site of phenazine N atoms, had the highest DNA cleavage activity and it cleaved DNA at the minimized concentra-

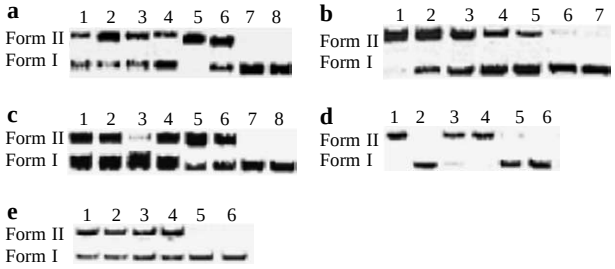

Figure 5. Photocleavage of closed supercoiled pBR322 DNA in Tris–HCl buffer (20 mM, pH 7.5) containing 20% acetonitrile. (a) DNA cleavage by **A1**–**A6** (100 μM) for 1 h. Lanes 1–6, **A6**, **A5**, **A4**, **A3**, **A2**, **A1** and DNA, respectively, lane 7, DNA alone (*hv*), and lane 8, DNA alone (no *hv*); (b) DNA cleavage by **A2** at various concentrations for 2 h. Lanes 1–5 **A2** at concentrations of 50, 20, 10, 5, and 1 μM, respectively, lane 6, DNA alone (*hv*), and lane 7, DNA alone (no *hv*); (c) DNA cleavage by **A2** (30 μM) in Tris–HCl buffer (20 mM, pH 7.5) for 2 h. Lanes 1–5, DNA and **A2** in the presence of DMSO, SOD (100 mg/mL), DTT (30 mM), ethanol (1.7 M), and histidine (6 mM), respectively, lane 6, DNA and **A2**, lane 7, DNA alone (*hv*), and lane 8, DNA alone (no *hv*); (d) mechanistic experiment for **A2** carried out in phosphate buffers (20 mM, pH 7.5) under aerobic conditions. DNA photocleavage by **A2** (30 μM) for 2.5 h. Lanes 1–3, DNA and **A2** in the presence of DMSO, DTT (30 mM), ethanol (1.7 M), respectively, lane 4, DNA and **A2**, lane 5, DNA alone (*hv*), and lane 6, DNA alone (no *hv*); (e) mechanistic experiment for **A2** carried out in phosphate buffers (20 mM, pH 7.5) under anaerobic conditions. DNA photocleavage by **A2** (30 μM) for 2.5 h. Lanes 1–3, DNA and **A2** in the presence of DMSO, DTT (30 mM), and ethanol (1.7 M), respectively, lane 4, DNA and **A2**, and lane 5, DNA alone (*hv*), lane 6, DNA alone (no *hv*).

tion of 1 μM (Fig. 5b). Compared to **A2**, **A3** with a methoxyl group at the 1-site and **A6** with a methyl group at the 4- site exhibited lower activities. These results showed that the two *peri* sites exerted different influences on DNA photo-cleaving activities. The order of their DNA cleaving abilities was: **A2** > **A5** > **A1** > **A4** > **A6** ≈ **A3**.

To verify the reactive species responsible for plasmid DNA cleavage, **A2** was chosen for the mechanistic experiment. As shown in Figure 5c, histidine (singlet oxygen quencher) and SOD (superoxide dismutase, superoxide anion scavenger) did not inhibit the DNA cleavage, DTT (dithiothreitol, superoxide anion scavenger), ethanol (radical killer) and DMSO (radical scavenger) inhibited the DNA damage to different extents, and DTT acted as the strongest inhibitor.

The inhibition of DNA cleavage by both ethanol and DMSO indicated that radicals might be involved in this process. It became known that the excited chromophore could oxidize the chloride anion (Tris–HCl buffer) to form the chloride radicals.[13] To exclude any 'heavy atom effect,' the same experiment was carried out with phosphate buffers (Fig. 5d). The results showed that both DMSO and ethanol did not inhibit DNA cleavage anymore, which indicated that the radicals resulted from the chloride anion in the Tris–HCl buffer.

The inhibition of DNA cleavage by DTT has suggested, that superoxide anions are likely to be involved in this DNA photocleavage process. As we know, the irradiated naphthalimide chromophore could damage the DNA via electron transfer[3] and the exited phenazine unit[14] could abstract H atoms from the environment. In addition, compounds with a C=N bond in aromatic rings usually photocleaved DNA via electron transfer or a H-abstraction mechanism[3] due to the generation of photo-excited $^3(n–\pi^*)$ and/or $^3(\pi–\pi^*)$ states. Moreover, a superoxide anion could be produced during the electron transfer process, in which the electrons first get transferred from nucleobases to intercalators and then to the oxygen. It should be noted that addition of SOD did not obviously inhibit the DNA cleavage as DTT did. This observation however did not rule out the possibility that a superoxide anion was involved in the DNA-cleaving process. It is on account of the hydrogen peroxide produced by SOD from the superoxide anion under photo-irradiation, which then contradicted the inhibition of superoxide anion by SOD.

To illustrate further the existence of electron transfer process, a mechanistic experiment was performed under anaerobic conditions. In this experiment, a phosphate buffer was used to prevent the 'heavy atom effect.' Figure 5e clearly shows that DTT did not inhibit the DNA cleavage anymore under anaerobic conditions. However, the supercoiled pBR322 DNA was still damaged, although not as effectively as it was under aerobic conditions. This result shows that superoxide anion was likely to be a 'side-product' of the electron transfer process under aerobic conditions. In addition, the electron transfer process favored the DNA damage more than the superoxide anion, which could be deduced from the DNA form II/form I ratio under aerobic/anaerobic conditions.

3. Conclusion

In summary, this study has demonstrated the design of novel DNA intercalative isoquinolino[5,4-*ab*]phenazine derivatives **A1**–**A6** and the evaluation of their biological activities. The two *peri* sites of phenazine N atoms played different roles on these bioactivities. At 100 μM, all these compounds (but **A2** and **A6**) inhibited the activity of topoisomerase I. **A6** showed efficient activities against both A549 and P388. **A1**, **A5**, and **A6** exhibited selective cytotoxicity against P388. There was no obvious connection between the cytotoxic potency of **A1**–**A6** and their topoisomerase I inhibitory activities. Under the irradiation of 365 nm-UV light, the circular supercoiled pBR322 could be cleaved by **A2** at the lowest concentration of 1 μM. Under anaerobic conditions, the electron transfer mechanism contributed mainly to the DNA cleavage while the superoxide anion also involved in this process under aerobic conditions.

4. Experimental

4.1. Materials

All the solvents were of analytical grade. ^{1}H NMR was measured on a Bruker AV-400 spectrometer, with chemical shifts reported as parts per million (in DMSO-d_6/$CDCl_3$, TMS as an internal standard). Mass spectra were measured on a HP 1100 LC–MS spectrometer. Melting points were determined with an X-6 micro-melting point apparatus and are uncorrected. Absorption spectra were determined on a PGENERAL TU-1901 UV–vis Spectrophotometer.

5. Synthesis

5.1. Synthesis of A1

(a) 4-Bromo-3-nitro-1, 8-naphthalic anhydride (3.22 g, 10 mmol) and aniline (1.1 g, 11.8 mmol) were added to 7 mL DMF. The reaction mixture was stirred at room temperature for 5 h, then cooled and poured into the ice water, filtered, and dried. The crude product was obtained as an orange solid (2.84 g, 8.5 mmol, 85% yield). APCI-MS (positive) *m*/*z*: 335.1 ($[M+H]^+$). (b) 4-aniline-3-nitro-1, 8-naphthalic anhydride (2 g, 5.81 mmol) and $NaBH_4$ (1 g, 26.3 mmol) were dissolved in 100 mL of 2 M NaOH solution. The solution was refluxed for 24 h and then cooled, and HCl was added until the pH became 6. Then, the mixture was filtered and dried to give a red product. The red product was suspended in boiling MeOH, and then sufficient Et_3N was added to just give a homogeneous solution. After being acidified with AcOH, the precipitate was filtered and dried (1.2 g, 3.9 mmol, 65% yield). This product was

not purified and was directly used in the next step. (c) 0.6 g of above-obtained solid was refluxed with *N*,*N*-dimethylethylenediamine (0.3 mL) in ethanol (30 mL) for 2 h, cooled, solvent removed, and separated on silica gel chromatography to yield the pure product.

Separated on silica gel chromatography ($CHCl_3$/MeOH = 9:1, v/v) to give pure $\mathbf{A}_1$ (0.629 g, 85% yield). **A1**: mp: 198.3–198.5 °C. ^{1}H NMR ($CDCl_3$) δ (ppm): 2.60 (s, 6H, NCH_3), 2.99 (s, 2H, NCH_2), 4.51 (s, 2H, $CONCH_2$), 7.96–8.08 (m, 3H), 8.38–8.43 (m, 2H), 8.76–8.79 (d, J = 8.0 Hz, 1H), 9.22 (s, 1H), 9.69–9.71 (d, J = 8.0 Hz, 1H), ESI-HRMS: Calcd for $C_{22}H_{18}N_4O_2$ ($M+H^+$): 371.1508, Found: 371.1510. IR (KBr): 2924, 2854, 1708, 1662, and 1336, cm^{-1}.

5.2. Synthesis of A2–A6

The preparation and purification procedure of **A2**–**A6** were similar to those of **A1**; different aniline derivatives were used here, instead of aniline.

Separated on silica gel chromatography ($CHCl_3$/MeOH = 9:1, v/v) to give purified **A4** (43% yield), **A5** (55% yield), and **A6** (35% yield). During the synthesis of **A2** and **A3**, two isomers at the 1-site and the 3-site were produced and 1-site isomer was the main product. The purified products could not be obtained after silica gel chromatography. So, recrystallization from ethanol after silica gel chromatography ($CHCl_3$/MeOH = 9:1, v/v) was necessary to give the purified **A2** (32% yield) and **A3** (40% yield).

A2: mp: 178.1–178.5 °C. ^{1}H NMR ($CDCl_3$) δ (ppm): 2.47 (s, 6H, NCH_3), 2.83 (s, 2H, NCH_2), 2.99 (s, 3H, CH_3), 4.43–4.46 (t, J_1 = 6.8 Hz, J_2 = 7.2 Hz, 2H, $CONCH_2$), 7.77–7.79 (d, J = 6.4 Hz, 1H), 7.86–7.90 (t, J_1 = 8.0 Hz, J_2 = 7.6 Hz, 1H), 8.01–8.05 (t, J_1 = 7.6 Hz, J_2 = 7.6 Hz, 1H), 8.22–8.24 (d, J = 8.4 Hz, 1H), 8.75–8.77 (d, J = 7.6 Hz, 1H), 9.24 (s, 1H), 9.66–9.68 (d, J = 8.0 Hz, 1H), ESI-HRMS: Calcd for $C_{23}H_{20}N_4O_2$ ($M+H^+$): 385.1665, Found: 385.1671. IR (KBr): 2924, 2853, 1702, 1660, 1340 cm^{-1}.

A3: mp: 189.6–190.5 °C. ^{1}H NMR ($CDCl_3$) δ (ppm): 2.99 (s, 6H, NCH_3), 3.52 (s, 2H, NCH_2), 4.24 (s, 3H, OCH_3), 4.70 (s, 2H, $CONCH_2$), 7.26–7.29 (t, J_1 = 7.6 Hz, J_2 = 8.0 Hz, 1H), 7.91–8.05 (m, 3H), 8.77–7.78 (d, J = 6.8 Hz, 1H), 9.39 (s, 1H), 9.69–9.71 (d, J = 8.4 Hz, 1H), ESI-HRMS: Calcd for $C_{23}H_{20}N_4O_3$ ($M+H^+$): 401.1614, Found: 401.1595. IR (KBr): 2924, 2853, 1702, 1660, 1340 cm^{-1}.

A4: mp: 209.6–210.1 °C. ^{1}H NMR ($CDCl_3$) δ (ppm): 2.49 (s, 6H, NCH_3), 2.72 (s, 3H, CH_3), 2.85 (s, 2H, NCH_2), 4.43–4.47 (t, 2H, J_1 = 6.8 Hz,J_2 = 7.2 Hz, $CONCH_2$), 7.82–7.84 (d, J = 10.0 Hz, 1H), 8.01–8.05 (t, J_1 = 7.6 Hz, J_2 = 8.0 Hz, 1H), 8.13 (s, 1H), 8.28–8.30 (d, J = 8.8 Hz, 1H), 8.74–8.76 (d, J = 7.2 Hz, 1H), 9.18 (s, 1H), 9.67–9.67 (d, J = 8.0 Hz, 1H), ESI-HRMS: Calcd for $C_{23}H_{20}N_4O_2$ ($M+H^+$): 385.1665, Found: 385.1664. IR (KBr): 2924, 2854, 1704, 1663, 1357 cm^{-1}.

A5: mp: 214.4–215.2 °C. ^{1}H NMR ($CDCl_3$) δ (ppm): 2.61(s, 6H, NCH_3), 3.01 (s, 2H, NCH_2), 4.09 (s, 3H, OCH_3), 4.51 (s, 2H, $CONCH_2$), 7.56–7.57 (d, J = 2.8 Hz, 1H), 7.65–7.65 (d, J = 2.4 Hz, 1H), 7.67–7.68 (d, J = 2.8 Hz, 1H), 8.01–8.05 (t, J_1 = 7.6 Hz,J_2 = 8.0 Hz, 1H), 8.26–8.28 (d, J = 9.6 Hz, 2H), 8.73–8.75 (d, J = 7.6 Hz, 1H), 9.16 (s, 1H), 9.63–9.65 (d, J = 8.0 Hz, 1H), ESI-HRMS: Calcd for $C_{23}H_{20}N_4O_3$ ($M+H^+$): 401.1614, Found: 401.1618. IR (KBr): 2924, 2853, 1705, 1655, 1350 cm^{-1}.

A6: mp: 185.2–185.5 °C. ^{1}H NMR ($CDCl_3$) δ (ppm): 2.98 (s, 6H, NCH_3), 3.06 (s, 3H, CH_3), 3.49 (s, 2H, NCH_2), 4.69 (s, 2H, $CONCH_2$), 7.83–7.86 (m, 2H), 8.05–8.09 (t, J_1 = 8.0 Hz, J_2 = 8.0 Hz, 1H), 8.20–8.22 (d, J = 6.8 Hz, 1H), 8.75–8.77 (d, J = 7.2 Hz, 1H), 9.23 (s, 1H), 9.73–9.75 (d, J = 8.8 Hz, 1H). ESI-HRMS: Calcd for $C_{23}H_{20}N_4O_2$ ($M+H^+$): 385.1665, Found: 385.1682. IR (KBr): 2924, 2854, 1704, 1667, 1345 cm^{-1}.

5.3. Spectroscopic measurements and DNA-binding studies

UV–vis absorption spectra were recorded on Shimadzu UV and fluorescent spectra on a Perkin-Elmer LS 50 luminescence spectrophotometer.

A2 was dissolved in absolute ethanol to give 10^{-5} M solutions and rhodamine B in ethanol was used as quantum yield standard.

DNA-binding studies were performed in Tris buffer (tris(hydroxymethyl)aminomethane)–HCl (20 mM, pH 7.0). 0.1 mL of **A2** DMSO solution (10^{-3}–10^{-4} M) was diluted with buffer to 10 mL. Fluorescent wavelength and intensity were measured.

5.4. Topoisomerase I inhibitory

Topoisomerase I was purchased from TaKaRa Co., Ltd. The cleavage assays were performed as reported in reference.[15] The drug, DNA, and topoisomerase I were incubated for 30 min at 37 °C in Tris–HCl buffer (20 mM, pH 7.5) before carrying out agarose-gel electrophoresis. 2% agarose-gel electrophoresis was carried out at 25 V in 40 mM TAE buffer (40 mM tris(hydroxymethyl)aminomethane, 30 mM glacial acetic acid, and 1 mM EDTA, pH 7.5). After electrophoresis, the gel was stained with ethidium bromide. The experiments were repeated three times.

5.5. Cytotoxicity in vitro evaluation

The prepared compounds were submitted to Shanghai Institute of Materia Medica with a view to get their cytotoxicities tested.

5.6. Photocleavage of supercoiled pBR322 DNA

Irradiation was performed with a lamp (365 nm), placed at 20 cm from the samples. The irradiated samples contained pBR322 DNA (0.5 μg) dissolved in Tris–HCl buffer (20 mM, pH 7.5) and the examined compounds.

Supercoiled DNA, nicked DNA, and linear DNA run at positions I, II, and III, respectively. The samples were analyzed by 1% agarose-gel electrophoresis. The agarose gel was stained with ethidium bromide.

Acknowledgments

Financial support by National Basic Research Program of China (2003CB114400) and under the auspices of 863 plan for High-Tech (2003AA2Z3520) is greatly appreciated. This work is also supported by Dalian Excellent Young Scientist Research Fund.

References and notes

1. Kochevar, E. D. D. In *Dunn in Bioorganic Photochemistry*; Morrison, H., Ed.; John Wiley: New York, 1990, pp 273–283.
2. (a) Laursen, J. B.; Nielsen, J. *Chem. Rev.* **2004**, *104*, 1663; (b) Rastogi, K.; Chang, J.-Y.; Pan, W.-Y.; Chen, C.-H.; Chou, T.-C.; Chen, L.-T.; Su, T.-L. *J. Med. Chem.* **2002**, *45*, 4485; (c) Wang, S.; Miller, W.; Milton, J.; Vicker, N.; Stewart, A.; Charlton, P.; Mistry, P.; Hardick, D.; Denny, W. A. *Bioorg. Med. Chem. Lett.* **2002**, *12*, 415; (d) Braña, M. F.; Ramos, A. *Curr. Med. Chem.: Anti-cancer Agents* **2001**, *1*, 237; (e) Rogers, J. E.; Weiss, S. J.; Kelly, L. A. *J. Am. Chem. Soc.* **2000**, *122*, 427; (f) Qian, X.; Huang, T. B.; Wei, D. Z.; Zhu, D. H.; Fan, M. C.; Yao, W. *J. Chem. Soc., Perkin. Trans.* **2000**, *2*, 715; (g) Rogers, J. E.; Kelly, L. A. *J. Am. Chem. Soc.* **1999**, *121*, 3854; (h) Braña, M. F.; Castellano, J. M.; Perron, D.; Maher, C.; Conlon, D.; Bousquet, P. F.; George, J.; Qian, X.-D.; Robinson, S. P. *J. Med. Chem.* **1997**, *40*, 449; (i) Saito, I.; Takayama, M.; Sugiyama, H.; Nakatani, K.; Tsuchida, A.; Yamamoto, M. *J. Am. Chem. Soc.* **1995**, *117*, 6406.
3. (a) Amitage, B. *Chem. Rev.* **1998**, *98*, 1171; (b) Saito, I.; Nakatani, K. *Bull. Chem. Soc. Jpn.* **1996**, *69*, 3007; (c) Hwu, J. R.; Lu, K. L.; Yu, S. F.; Yu, L. J.; Kumaresan, S.; Lin, K. J.; Tsay, S. C. *Photochem. Photobiol.* **2002**, *75*, 457; (d) Teulade-Fichou, M.-P.; Perrin, D.; Boutorine, A.; Polverari, D.; Vigneron, J.-P.; Lehn, J.-M.; Sun, J.-S.; Garestier, T.; Helene, C. *J. Am. Chem. Soc.* **2001**, *123*, 9283; (e) Rogers, J. E.; Le, T. P.; Kelly, L. A. *Photochem. Photobiol.* **2001**, *73*, 223; (f) Hurley, A. L.; Maddox, M. P.; Scott, T. L.; Flood, M. R.; Mohler, D. L. *Org. Lett.* **2001**, *3*, 2761; (g) Tsai, F. Y.; Lin, S. B.; Tsay, S. C.; Lin, W. C.; Hsieh, C. L.; Chuang, S. H.; Kan, L. S.; Hwu, J. R. *Tetrahedron Lett.* **2001**, *42*, 5733; (h) Cornia, M.; Menozzi, M.; Ragg, E.; Mazzini, S.; Scarafoni, A.; Zanardi, F.; Casiraghi, G. *Tetrahedron* **2000**, *56*, 3977; (i) Lorente, A.; Fernandez-Saiz, M.; Herraiz, F.; Lehn, J.-M.; Vigneron, J.-P. *Tetrahedron Lett.* **1999**, *40*, 5901.
4. Bousquet, P. F.; Braña, M. F.; Conlon, D.; Fitzgerald, K.; Perron, M. D.; Cocchiaro, C.; Miller, R.; Moran, M.; George, J.; Qian, X.-D.; Keilhauer, G.; Romerdahl, C. A. *Cancer Res.* **1995**, *55*, 1176.
5. Fernández, M. J.; Grant, K. B.; Herraiz, F.; Yang, X.; Lorente, A. *Tetrahedron Lett.* **2001**, *42*, 5701.
6. Gamage, S. A.; Spicer, J. A.; Rewcastle, G. W.; Milton, J.; Sohal, S.; Dangerfield, W.; Mistry, P.; Vicker, N.; Charlton, P. A.; Denny, W. A. *J. Med. Chem.* **2002**, *45*, 740.
7. Phillips, T.; Haq, I.; Meijer, A. J.; Adams, H.; Soutar, I.; Swanson, L.; Sykes, M. J.; Thomas, J. A. *Biochemistry* **2004**, *43*, 13657.
8. (a) Yang, Q.; Qian, X.; Xu, J. Q.; Sun, Y. S.; Li, Y. G. *Bioorg. Med. Chem.* **2005**, *13*, 1615; (b) Qian, X.; Li, Y. G.; Xu, Y. F.; Liu, D.; Qu, B. Y. *Bioorg. Med. Chem.* **2004**, *14*, 2665; (c) Xu, Y. F.; Qian, X.; Yao, W.; Mao, P.; Cui, J. *Bioorg. Med. Chem.* **2003**, *11*, 5427; (d) Qian, X.; Yao, W.; Chen, G.; Huang, X. Y.; Mao, P. *Tetrahedron Lett.* **2001**, *42*, 6175.
9. Rewcastle, G. W.; Denny, W. A.; Bruce, C. B. *J. Med. Chem.* **1987**, *30*, 843.
10. Gupta, M.; Ali, R. *J. Biochem.* **1984**, *95*, 1253.
11. Skehan, P.; Storeny, R.; Scudiero, D.; Monks, A.; McMahon, J.; Vistica, D.; Warren, J. T.; Bokesc, H.; Kenney, S.; Boyd, M. R. *J. Natl. Cancer Inst.* **1990**, *82*, 1107.
12. Kuroda, M.; Mimaki, Y.; Sashida, Y.; Hirano, T.; Oka, K.; Dobashi, A.; Li, H.; Harada, N. *Tetrahedron* **1997**, *53*, 11549.
13. Rogers, J. E.; Abraham, B.; Rostkowski, A.; Kelly, L. A. *Photochem. Photobiol.* **2001**, *74*, 521.
14. (a) Bailey, D. N.; Doe, D. K.; Hercules, D. M. *J. Am. Chem. Soc.* **1968**, *90*, 6291; (b) Japar, S. M.; Abrahamson, E. W. *J. Am. Chem. Soc.* **1971**, *93*, 4140.
15. Kim, J. S.; Sun, Q.; Yu, C.; Liu, A.; Liu, L. F.; LaVoie, E. J. *Bioorg. Med. Chem.* **1998**, *6*, 163.